CC-PGI: Imaging prompt gammas with Compton cameras

Dedicated Monte Carlo simulations and image reconstruction algorithms for range verification in particle therapy using Compton cameras

***J. Werner, J. Kasprzak, M. Rafecas**, Institute of Medical Engineering, Universität zu Lübeck*

In Short

- Particle therapy needs range verification methods to ensure the correct dose distribution in the tumor and better spare the surrounding healthy tissues.
- Compton cameras (CC) are under investigation as a tool for range verification in particle therapy.
- Accurate simulations of CCs and therapeutic particle beams based on Monte Carlo methods help to understand the physical processes and detector limitations for the specific application.
- To ensure a correct range verification with CCs, dedicated iterative image reconstruction algorithms are needed.

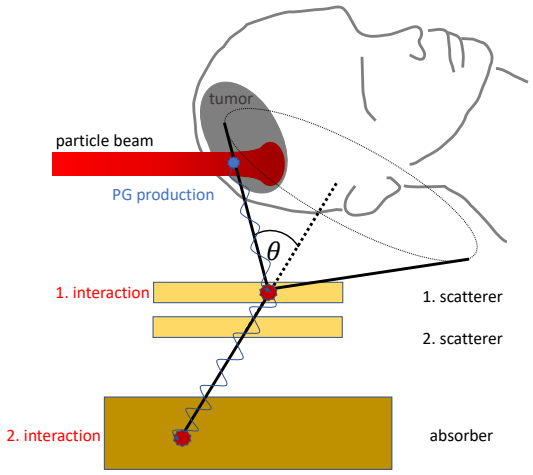

***Figure 1:** Principle of CC imaging. The PG is produced within the particle beam, is Compton scattered in the scatterer and then photoelectric absorbed in the absorber.*

Particle therapy is a widely accepted tumor treatment method, thanks to the well-defined penetration range of protons and heavier ions, as well as the maximum dose transfer at the end of this range. As a consequence, the tumor is radiated but the surrounding tissue can be spared. Unfortunately this beam range is susceptible to changes of the tissue composition along the beam path or to changes in the patient position between the daily radiation fractions. For this reason range verification methods are mandatory. At present, range deviations are mainly detected indirectly, making use of the secondary radiation derived from the treatment, like prompt gamma-rays (PG). PGs emerge from atomic nuclei few picoseconds after being excited by the beam particles. PGs are characterized by a broad energy spectrum up to several MeV, so that most PG leave the patient body and can be detected. Compton cameras (CC) have been proposed to detect PG radiation. By means of tomographic reconstruction algorithms applied to CC data, a three-dimensional image of the PG emission origins can be generated. As this distribution is correlated to the beam extent, possible range deviations can be identified by inspecting the reconstructed images.

Compton cameras rely on the particular features of the Compton effect. In the ideal case, the incoming photon undergoes a Compton interaction in the front detector layers, the so-called *scatterers*; subsequently, the scattered photon is photoelectrically absorbed in another detector layer, the *absorber*. Using the information related to the two interactions, the origin of the photon can be restricted to a half-cone, where the first interaction position defines the cone vertex. Using Compton kinematics the cone half-angle θ, which complies with the Compton scattering angle, can be calculated as:

$$\cos(\theta) = 1 - m_e c^2 \cdot \frac{E_1}{E_2(E_1 + E_2)}; \qquad (0.1)$$

E_1 and E_2 are the deposited energies under the assumption that the initial energy was $E_0 = E_1 + E_2$. Fig. 1 shows the described principle of CC-PG imaging. An event, or coincidence, includes all interactions that were detected within a certain coincidence time window between the detector layers.

Monte Carlo (MC) simulations play an important role in the design and optimization of detector systems, as well as in the evaluation of image reconstruction methods and the calculation of physical models. With the help of MC methods, the whole chain can be described, from particle production and beam irradiation to the detection of secondary radiation by the range-verification detectors. Through this chain we are able to produce data for reconstruction and to validate the designed algorithms. In this project, the *Geant4 Application for Emission Tomography* toolkit (GATE) is used [1].

To visualise the 3D distribution of radiation sources like the origins of the PG resulting from the irradiation, tomographic reconstruction is needed. The most commonly used algorithms in CC imaging is the *List Mode Maximum Likelihood Expectation*

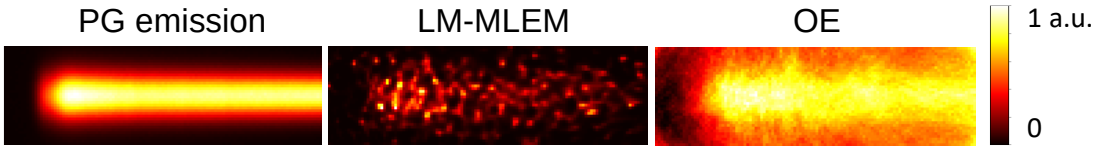

Figure 2: *Reconstructed images. The first column shows the PG emission, i.e. the output from a Monte Carlo simulation that serve as reference. Column two and three show the images reconstructed with LM-MLEM and OE, respectively.*

Maximization (LM-MLEM) algorithm. LM-MLEM is based on the maximization of an objective function, the Poisson likelihood. Given M events, LM-MLEM provides an iterative refinement of the current image estimate in voxel j, $f_j^{(n)}$, as:

$$f_j^{(n+1)} = \frac{f_j^{(n)}}{s_j} \sum_{i=1}^{M} \frac{a_{ij}}{\sum_{j'=1}^{N} a_{ij'} f_{j'}^{(n)}}, \qquad (0.2)$$

where s_j and a_{ij} are elements of the so-called sensitivity and system matrix, respectively: s_j corresponds to the detection probability of a PG emitted from voxel j, and a_{ij} describes the probability that a PG originating from j is detected as the i-th event.

The *Origin Ensemble* (OE) algorithm has also attracted attention for CC image reconstruction. OE uses the Metropolis-Hasting algorithm to estimate the expected value of the PG emission distribution conditioned on the measured data. The algorithm generates a sequence of samples of the emission distribution (aka *states*) following a Markov chain. To create the initial state, an emission origin is randomly assigned to each event of the list.

Next, a new origin is proposed to each event i; this event is reassigned to the new origin according to the acceptance probability from state X to state X':

$$A(X \to X') = \min\left(1, \frac{a_{ij'}\ s_j\ (x_{j'}+1)}{a_{ij}\ s_{j'}\ (x_j)}\right), \qquad (0.3)$$

where x_j is the event density in voxel j in the current state X. The reconstructed image is obtained by averaging over several states, starting after the Markov chain has reached the equilibrium.

Fig. 2 shows the true PG distribution as well as the reconstructed images with LM-MLEM and OE [3]. The high level of noise present in the LM-MLEM image is caused by the very low event statistics. "Night sky" artefacts are indeed typical for low-count MLEM reconstruction when the algorithm runs until convergence. In contrast, OE yields blurred images, as a consequence of averaging over many noisy states. Both cases show that noise regularization is mandatory. To this aim, our current work focuses on exploiting a-priori information within a Bayesian perspective. We are inspecting several *priors* for penalized MLEM [4] and OE.

Exemplary results for OE are shown in Fig. 3; here a cylindrical activity source was simulated and reconstructed by means of OE with the *Quadratic Gibbs prior* (Q-OE) and *Total-Variation Gibbs prior* (TV-OE). The *Flat prior* (F-OE) serves as a reference. Both Q-OE and TV-OE allowed the background noise to be significantly reduced for the specified value of the parameter β.

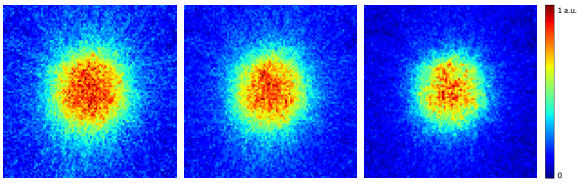

Figure 3: *Tranversal views of the reconstructed images at the center of the cylinder The image grid consisted of* $100 \times 100 \times 100$ *voxels, size:* $1\ mm^3$.

Thanks to the HLRN, it is possible to run realistic simulations with different settings (e.g. various source distributions, different photon or proton beam energy, etc.) We can also run multiple realizations of each configuration and study the statistical properties of our results. Moreover, this infrastructure also allows us to study in depth the effects on the reconstructed images of the weighting assigned to the priors as well as other free parameters.

WWW

https://www.imt.uni-luebeck.de/research/nuclear-imaging.html

More Information

[1] http://www.opengatecollaboration.org/

[2] Etxebeste, A, et al, Phys. Med. Biol 65 (2020): 055004, doi: doi:10.1088/1361-6560/ab6529

[3] Kohlhase, N, et al, TRPMS 4 (2020): 233, doi: doi: 10.1109/TRPMS.2019.2937675

[4] Kohlhase, N et al. 2020 IEEE NSS/MIC, doi: 10.1109/NSS/MIC42677.2020.9507820

Funding

DFG Research Grant no. 383681334.

DFG Subject Area

205-32